Published in final edited form as:
*Biomaterials*. 2011 April ; 32(10): 2479–2488. doi:10.1016/j.biomaterials.2010.12.010.

# Ruthenium-catalyzed photo cross-linking of fibrin-based engineered tissue

**Jason W. Bjork**[a], **Sandra L. Johnson**[a], and **Robert T. Tranquillo**[a,b]

[a]Department of Biomedical Engineering, University of Minnesota 7-105 Nils Hasselmo Hall 312 Church St. Minneapolis, MN 55455

[b]Department of Chemical Engineering and Materials Science, University of Minnesota 151 Amundson Hall 421 Washington Ave. SE Minneapolis, MN 55455

## Abstract

Most cross-linking methods utilize chemistry or physical processes that are detrimental to cells and tissue development. Those that are not as harmful often do not provide a level of strength that ultimately meets the required application. The purpose of this work was to investigate the use of a ruthenium-sodium persulfate cross-linking system to form dityrosine in fibrin-based engineered tissue. By utilizing the tyrosine residues inherent to fibrin and cell-deposited proteins, at least 3-fold mechanical strength increases and 10-fold stiffness increases were achieved after cross-linking. This strengthening and stiffening effect was found to increase with culture duration prior to cross-linking such that physiologically relevant properties were obtained. Fibrin was not required for this effect as demonstrated by testing with collagen-based engineered tissue. Cross-linked tissues were implanted subcutaneously and shown to have minimal inflammation after 30 days, similar to non-cross-linked controls. Overall, the method employed is rapid, non-toxic, minimally inflammatory, and is capable of increasing strength and stiffness of engineered tissues to physiological levels.

## Introduction

Many tissue engineering applications utilize biological polymers as a cell scaffold, including applications ranging from bone [1] or cartilage replacement [2] to cardiovascular tissue replacements [3, 4]. Biological polymers – such as collagen, and fibrin among others – have the advantages of possessing cell-binding properties [5], becoming aligned during tissue fabrication in vitro [6, 7], being remodeled by natural enzymatic processes, and inducing less inflammation than many degradation reactions in synthetic polymer systems [8]. For many applications, however, the strength and stiffness of the resulting tissue do not meet the requirements for in vivo transplantation.

One method to improve the strength of biopolymers lies with the formation of covalent cross links within and between the polymer chains or fibrils associated with polymer assembly. For example, research has been conducted to cross-link collagen using glutaraldehyde [9],



Address correspondence to Robert T. Tranquillo 151 Amundson Hall 421 Washington Ave. SE Minneapolis, MN 55455. Phone: 612-625-6868 Fax: 612-626-6583 tranquillo@umn.edu.

diimidoesters [10], UV light [11, 12], and sugars such as ribose [13]. Other research evaluated modification of the collagen molecule with photo-chemical cross-linkers by mixing collagen with synthetic cross-linkers [10, 14, 15]. Fibrin has also been the subject of cross-linking research, being cross-linked by glutaraldehyde [16], bifunctional carbodiimide [17] or genipin [18] as well as exposure to UV light [19]. Cross-linking methods are typically applied to collagen or fibrin as hydrogel scaffolds prior to cell seeding and formation of engineered tissue [15, 17, 19], though research has also recently been conducted to crosslink these materials in the presence of cells [14].

While increased strength and stiffness typically result, several issues arise with these methods. First, cross-linking chemically, such as with glutaraldehyde, often results in a tissue or scaffold that tends to be cytotoxic or otherwise detrimental upon implantation [16]. Since chemical cross-linking must then be done in the absence of cells to avoid toxicity, the cells must be seeded after cross-linking and a uniform distribution of cells throughout the scaffold is not obtained. Second, conjugation of photo-polymerizable molecules and subsequent polymer initiation can result in residual monomers in a scaffold, which again lead to cytotoxic conditions. Lastly, polymerization by UV light also has cytotoxic effects on cells. While short exposure times could potentially be tolerated, acceptable polymerization yields often require UV exposure of 10 minutes or longer, which results in loss of cell viability [15, 20]. Though these methods are not without utility, a cross-linking method that allows a homogeneous distribution of cells to be present during cross-linking that yields physiologic strength and stiffness without toxic effects is desirable.

Fancy & Kodadek proposed a method to form dityrosine bonds between proteins [21] and Elvin et al. extended these findings to fibrinogen [22, 23]. This method is based on ruthenium II trisbipyridyl chloride ($[RuII(bpy_3)]^{2+}$) and sodium persulfate (SPS). The proposed mechanism suggests that these reagents, in the presence of blue light, form Ru(III) and a sulfate radical. These intermediates form tyrosine radicals, which then form a dityrosine cross-link [21]. Elvin et al. demonstrated that this chemistry forms dityrosine cross-links in fibrinogen [22]. Since fibrinogen is inherently rich in tyrosine, this method requires no modification of the protein. Furthermore, this method utilizes blue light rather than UV, which avoids the effects of short wavelength light and the reagent concentrations required are not toxic to cells [21, 22, 24]. Utilization of $[RuII(bpy_3)]^{2+}$ was subsequently shown to cross-link fibrin and to stiffen fibrin-based tissue constructs to control the level of cell-induced compaction without impacting collagen deposition or mechanical properties after conditioning in a bioreactor [24].

In this work, the $[RuII(bpy_3)]^{2+}$ / SPS cross-linking chemistry was applied to fibrin and collagen-based tubular tissue constructs after varied culture durations. Over time these constructs were compacted by cell traction forces while extracellular matrix (ECM) molecules, such as collagen and fibronectin, were deposited [25]. These protein materials have the potential to form dityrosine cross-links based on their tyrosine content [26]. It was hypothesized that the remodeling process would serve to increase the density or cross-linkable proteins and thereby increase the probability of forming a dityrosine bond between fibers during the cross-linking process, which would, in turn, yield improved mechanical properties. Tubular tissue constructs were characterized by tensile testing and burst pressure to compare cross-linked versus non-cross-linked samples, as well as biochemical and ultrastructural analysis by histology and scanning electron microscopy. Further, these materials were examined in a subcutaneous implantation study to understand the innate inflammatory response to cross-linked fibrin-based tissue.

## Materials and Methods

### Cell Culture

Neonatal human dermal fibroblasts (nhDFs, Clonetics) were maintained in DMEM/F12 with 15% fetal bovine serum (FBS) and 1% penicillin/streptomycin (Invitrogen) on tissue culture plastic in a 5% $CO_2$, 37°C incubator. Cells were split at near 100% confluence and harvested for use at passage 9.

### Tubular Tissue Construct Fabrication & Culture

Fibrin-based tissue constructs were prepared as previously described [7, 25]. Briefly, fibrinogen (Sigma), cells and thrombin (Sigma) were mixed in a 4:1:1 ratio to achieve a final concentration of 3 mg/mL and $0.5 \times 10^6$ cells/mL. This mixture was then injected into a tubular mold housing a 2 mm glass mandrel that was pretreated with Pluronic F-127 (Sigma) to minimize gel adhesion. Fibrin gels were allowed to form vertically for 30 minutes prior to removal from the mold into a standard 15 cm culture dish. Culture medium consisted of DMEM (Gibco) supplemented with 10% FBS, 50 μg/mL ascorbic acid, and 2 μg/mL insulin, 1% penicillin/streptomycin and 0.25 μg/mL amphotericin B.

Collagen-based constructs were prepared based on previous methods [27]. 3.4 mL 1 M HEPES, 624 μL 1 M NaOH, 2.4 mL 10× MEM (Sigma), 1.44 mL FBS, and 240 μL L-glutamine (Gibco) were rapidly mixed with 15.5 mL acid extracted rat tail collagen (Invitrogen) while kept cold. This mixture was cast into a mold, and then the gels were incubated at 37°C for 45 minutes and cultured under similar conditions.

### Ruthenium Catalyzed Cross-Linking

Stock solutions of $[RuII(bpy)_3]^{2+}$ and SPS (both from Sigma) were prepared by dissolution in distilled water, yielding solutions of 15 and 47.5 mg/mL, respectively. Stock solutions were made fresh for each cross-linking experiment. These were diluted with phosphate buffered saline (PBS) to yield a solution of 1.5 mg/mL $[RuII(bpy)_3]^{2+}$ and 2.4 mg/mL SPS. Constructs were individually incubated in this solution for 10 minutes, after which blue light ($\lambda$ = 458 nm) was delivered with a custom mesh of LEDs (Kingbright) from a distance of approximately 3 cm, which provided a luminous intensity of 144 candela (28 mW/cm$^2$) as previously described [24]. An exposure time of 10 seconds was used unless specifically noted otherwise. Controls were similarly exposed to blue light but in the absence of the cross-linking agents.

### Uniaxial Tensile Testing

Dimensions of tissue rings were taken prior to mechanical loading. Width and length were measured with digital calipers (Mitutoyo). Thickness was measured using a 50-g force probe attached to a displacement transducer. The rings were placed onto a T-bar apparatus that was submerged in PBS and stretched uniaxially using a Microbionix (MTS Systems) to obtain circumferential tensile mechanical properties. Rings were straightened with a 5 mN load to serve as the reference length. 6 cycles of 0–10% strain were used to precondition the rings, followed by stretch to failure at 2 mm/min. True strain was calculated based on the change in length of the rings during the test, while engineering stress was calculated as measured force divided by initial cross-sectional area. The modulus was determined by linear-regression of a portion of the stress-strain curve taken from after the toe region to the point of tissue failure.

### Burst Pressure Testing

Constructs were removed from the mandrel and mounted with silk suture onto hose barb luer adapters. A syringe pump (Harvard Apparatus) was used to drive PBS through the system to remove air bubbles, after which the distal end of the system was closed to pressurize the tissue. An in-line pressure transducer (Omega) upstream of the construct was used to monitor the pressure, which was recorded using LabVIEW (National Instruments). PBS was then injected at a constant rate of 2 ml/min until failure. The burst pressure was recorded as the maximum pressure prior to failure.

### Collagen and Cell Quantification

A modified ninhydrin-based assay was used to quantify total protein [28]. A hydroxyproline assay was used to estimate collagen deposition in fibrin-based constructs [29]. Measured levels of 4-hydroxyproline are then converted to collagen using a conversion factor of 7.46 μg collagen per μg of 4-hydroxyproline. Cell number within the constructs was determined using a total DNA assay [30] and a conversion factor of 7.6 pg DNA per cell.

### Subcutaneous Implantation

Fibrin-based constructs were cultured for 7 weeks as described above. Prior to implant, samples were cross-linked, sectioned into 3 mm rings, and then maintained in lactated Ringer's solution until implanted. Implantation was conducted by placing an athymic (nude) rat ventrally on a surgical table. After being sterilely draped, six skin incisions were made, three each on the left and right sides of the spinal column. At each incision, a pocket of approximately one centimeter was made under the skin lateral to the spine using blunt dissection, into which a cross-linked or control sample was placed. The rats were euthanized at days 3, 7 and 30 for sample tissue explantation. Harvested samples were immediately placed in 10% neutral buffered formalin until paraffin embedding and histological sectioning. Sectioned samples were stained with hematoxylin and eosin (H&E), Masson's trichrome, and von Kossa stain. All procedures and animal care were conducted according to University of Minnesota IACUC-approved protocols.

### Histology

Constructs not implanted were fixed with 4% paraformaldehyde for 3 hours, rinsed, infiltrated with a solution of 30% sucrose, 5% DMSO in PBS, frozen in OCT, and then sectioned into 9 μm sections. Staining consisted of Lillie's trichrome and diaminobenzidine (DAB) immunostaining. Anti-fibronectin (Abcam) and anti-fibrinogen (American Diagnostica) polyclonal primary antibodies were used with HRP-conjugated secondary antibodies. After incubation with secondary antibodies, samples were incubated with DAB then counterstained with hematoxylin. Images were taken with 10× or 20× objectives.

### Scanning Electron Microscopy

Samples for SEM imaging (not antibody labeled) were fixed using a modified Karnovsky's fixation – 0.1 M sodium cacodylate containing 2% paraformaldehyde (PFA), 2.5% glutaraldehyde and 2 mM $CaCl_2$ for 3 hours at room temperature with continual mixing. Samples were post-fixed with 1% $OsO_4$ in cacodylate buffer for 1 hour then dehydrated in a graded ethanol series. Then, samples were freeze fractured in liquid $N_2$ to expose the cross-section region. Specimens were further dehydrated with absolute ethanol, critical point dried, mounted on aluminum stubs, and sputter coated with platinum to an approximate thickness of 2 nm. Images were acquired with a Hitachi S-900 Field Emission Scanning Electron Microscope at 3–5 keV.

Samples that were immunogold labeled were initially fixed for 10 minutes in 0.1% glutaraldehyde, followed by an additional 2 hours in modified Karnovsky's and post-fixed in 1% $OsO_4$. Samples were blocked with glycine and donkey serum, then labeled with anti-fibrinogen antibody (American Diagnostica) and 12 nm gold-labeled secondary, fixed again with the modified Karnovsky's and 1% $OsO_4$ steps and processed as above.

### Statistics

All data are presented as mean ± SEM with sample size denoted in figure captions. Statistical significance was determined by paired t-tests when paired comparisons were analyzed; otherwise, general linear model ANOVA analysis was conducted using a Bonferroni post-hoc test. All statistical analysis was conducted using Minitab 15.

## Results

### Effect of Cross-Linking and Culture Duration on Mechanical Properties

Fibrin gels containing neonatal human dermal fibroblasts (nhDFs) were cultured and tested at intervals ranging from 1 to 11 weeks. At the time of tissue harvest, constructs were cut in half. One half served as the control and was maintained in PBS while the other half was cross-linked according to the procedure outlined in the Materials and Methods section and is pictured in Figure 1. Figure 2 A and B show that there was no improvement in the ultimate tensile strength (UTS) or modulus when the cross-linking was done after 1 week of culture. However, when cross-linking was done after 3 weeks of culture there was a 3-fold or greater increase in both UTS and modulus. The modulus increased 8-fold at 5 weeks of culture. The fold-increase in modulus was diminished after 5 weeks; however, the modulus approached 20 MPa when cross-linking was done after culturing for 11 weeks. The shaded region on Figure 2 A and B indicate measured UTS and modulus values for native rat aorta, which demonstrates that tissues cross-linked using this method have comparable strength and stiffness to native arterial tissues. Burst pressure testing was conducted on these samples, and burst pressures of over 1000 mmHg were measured for some tissues approximately 100 μm thick after cross-linking, a significant 3-fold increase over the paired non-cross-linked samples (Figure 2C).

### Effect of Cross-Linking Photo-Exposure Time on Mechanical Properties

The blue light exposure time was varied from 3 to 60 seconds to assess the impact of exposure time on strength and stiffness properties using constructs cultured for 4 weeks. As shown in Figure 2 D and E, there were improvements in mechanical properties with increasing exposure time up to 10 seconds. Control samples had an average UTS and modulus of approximately 200 kPa and 500 kPa, respectively. Control samples consisted of placing tissue in $[RuII(bpy_3)]^{2+}$ and SPS with no blue light exposure (no blue light control, denoted “0” in Figure 2 D and E). A secondary experiment evaluated maintaining tissue in PBS and exposing samples to blue light for up to 60 seconds (no cross-linking chemistry control, denoted “- Ru” in Figure 2 D and E). The UTS values increased nearly 4-fold after 10 seconds of blue light exposure, while the modulus increased over 10-fold for these samples.

### Effect of Cross-Linking on Mechanics of Digested Fibrin-based Tissues and Collagen-based Tissues

To evaluate the impact of fibrin degradation or, further, the absence of fibrin altogether, on cross-linking efficacy, constructs were treated with an overnight digestion in trypsin or initially cast using collagen rather than fibrin. In the case of trypsin-digested tissue, the fibrin-based constructs were cultured for 10 weeks. Prior to harvest, samples were digested

overnight at 37°C in 0.25% trypsin-EDTA and then cross-linked. Controls were maintained in an identical solution that did not have any trypsin. As shown in Figure 3 A and B, digested tissue exhibited significantly lower strength and stiffness compared to undigested tissue, as expected. However, a positive effect of cross-linking was still present. For digested samples, the UTS increased nearly 6-fold. Indeed, the strength of digested, cross-linked samples was not different from the non-digested control tissue. Further, the modulus of digested tissue increased nearly 50-fold after cross-linking.

Similar trends were observed for collagen-based tissue that was cultured for 4 weeks. As shown in Figure 3 C and D, the UTS increased approximately 3-fold for both UTS and modulus for these constructs, which demonstrates that fibrin is not required to achieve the benefits of this cross-linking method.

### Cell-induced Changes to Surrounding ECM During Culture

The fibrin-based tissue becomes significantly stronger and stiffer over time due to the accumulation of cell-deposited matrix (the majority of which is collagen), matrix densification and inherent enzymatic cross-linking [7, 25]. As shown in Figure 4A, the total protein concentration increased from 3 mg/mL, which was the initial fibrin concentration when the gels were cast, to approximately 120 mg/mL at 9 weeks of culture and beyond. At the later stages of culture, collagen accounted for 66% of the total protein (Figure 4B). Figure 5 shows the overall progression of ECM compaction and the qualitative increase in collagen content within the construct, and it also demonstrates that fibrin and fibronectin were present throughout the culture, even after 11 weeks. Figure 6 shows that these proteins, or at least fragments of these proteins, remained present after trypsin digestion. Both of these proteins are potentially important to the formation of dityrosine cross-links since they are each comprised of approximately 4% tyrosine [26] and thus could contribute to the change in strength observed after cross-linking. ECM was found to envelope collagen fibrils in the tissue, as shown in Figure 7A. The ECM in Figure 7A was co-located with fibrin staining in Figure 5 and was further identified to include residual fibrin by immunogold labeling of fibrin/ogen followed by SEM backscatter electron imaging as shown in Figure 7 D and E. Significant levels of additional ECM were not apparent in collagen-based tissue, as shown in Figure 7C.

### Subcutaneous Implant of Cross-Linked Fibrin-based Tissues

Subcutaneous implantation was conducted to compare the innate inflammatory response of cross-linked versus non-cross-linked tissue and evaluate possible calcification prior to use in other cardiovascular models. Athymic nude rats were utilized to avoid inflammation induced by MHC mismatch from xenotransplantation. As shown in Figure 8, an inflammatory fibrous capsule was observed after 3 days. After 7 days post-surgery, the relative level of inflammation was markedly reduced and comparison of control versus cross-linked tissue shows a slightly thicker fibrous capsule around the cross-linked samples. At 30 days, the engineered tissue had integrated into the host tissue in some regions, and the reactive layer around the tissue was further diminished in thickness. In most locations, no signs of inflammation were present. Furthermore, evidence of capillary formation was observed after 30 days in both cross-linked and control tissues, demonstrating host-cell infiltration and vascularization. Assessment of these samples showed a minimal inflammatory response overall for both the cross-linked and control samples.

## Discussion

This study demonstrates a rapid, non-cytotoxic method to significantly increase the mechanical strength and stiffness of engineered tissue by ruthenium-catalyzed cross-linking.

After sufficient cell-induced compaction of the surrounding tissue, which started as fibrinogen, $[RuII(bpy_3)]^{2+}$ catalyzed cross-linking yielded increases in UTS of up to 4-fold depending on the amount of time in culture. Increases in modulus of up to 10-fold were observed in some cases as well. These effects translated well to burst pressure testing, which is a standard functional test for engineered vascular tissue. A 3-fold increase was observed in burst pressures for cross-linked samples, with several samples exceeding 1000 mmHg. It is noteworthy that these tissue samples were approximately 100 μm at the time of testing, thus thicker samples have potential to provide higher burst pressures.

Previous studies have shown that cross-links are formed between tyrosine residues inherent to some biopolymers, such as fibrinogen, to form a covalent dityrosine bond [22–24]. Thus, this method requires no molecular functionalization to form the dityrosine cross-links. In addition to fibrin, other ECM proteins are capable of forming dityrosine. Proteins such as fibronectin, fibrillin, and matrix-associated glycoprotein (MAGP) each have a tyrosine content of over 3%, with MAGP near 6%. Elastin, a fibrillated ECM protein of interest in vascular tissue, could also contribute to ECM cross-linking. This study, however, was not optimized for elastin production, as levels of this protein were typically 0.5% or less of the total protein (additional ECM proteins of interest are shown in supplemental Figure S1) [26]. Collagen provides significant strength to the ECM and it can also potentially form dityrosine cross-links, though its tyrosine content is lower at approximately 1% [26]. Though these proteins have tyrosine in their amino acid sequence, their quaternary structure must also be amenable to tyrosine availability. This aspect was not a focus of this study; however, some reasonable proportion of tyrosine was available in order to achieve the observed improvements in mechanical properties.

Biopolymers such as collagen and fibrin have a multi-scale composition of fibrils comprised of monomers. Thus, cross-links could potentially form either between fibrils or within a fibril. Interestingly, when constructs were cross-linked after 1 week of culture, there was no change in strength or stiffness. Longer culture durations, after additional cell-induced compaction and ECM deposition, yielded significant improvements in these mechanical properties. This suggests that inter-fibril cross-links provide the primary contribution to observed enhancements rather than intra-fibril cross-links.

Deposition of collagen imparted increased strength and stiffness in non-cross-linked samples, as shown in Figure 2 A and B. In addition, cell-induced compaction of the ECM resulted in an increased protein concentration (Figure 4) and thus the potential for cross-link formation increased. Furthermore, the ECM proteins present in these constructs contained fibrin and fibronectin (Figure 5), each of which contains a relatively high amount of tyrosine. This combination of effects provides a plausible explanation for the significant increases in mechanical strengthening and stiffening observed after greater culture times and cross-linking.

Though fibrin has an abundance of tyrosine residues in its molecular structure, experimentation with collagen tubular constructs demonstrated that alternative protein scaffold materials can also yield improved mechanical properties. When collagen-based constructs were cultured similarly to fibrin-based constructs, entrapped cells compacted the matrix in these constructs as well. There was clearly no fibrin in these constructs but fibronectin was present as shown in Figure 5 A and G. Though no fibrin was present, the proximity of other cell-deposited proteins or fibers along with the collagen yielded dityrosine cross-links within collagen-based constructs such that after cross-linking a 3-fold increase in UTS and modulus was observed. The impact of residual fibrin cannot be discounted, however, as evidenced by the significant strength and stiffness observed in fibrin-based tissue after cross-linking.

Trypsin-digested fibrin-based tissue also demonstrated strength and stiffness increases after cross-linking. Trypsin digestion leaves collagen fibers largely intact, but many other ECM proteins are cleaved by this serine protease. After overnight digestion, the mechanical properties were markedly degraded; however, there were apparently enough residual protein fragments to enhance the UTS and modulus upon cross-linking compared to digested, non-cross-linked controls as shown in Figure 3. Figure 6 shows positive staining for fibrin and fibronectin in the trypsin-digested fibrin-based tissues, which demonstrates that degraded proteins could form cross-links within the ECM. This applies to constructs cultured under standard conditions since, after extensive remodeling of the fibrin and cell-deposited ECM during culture, the protein fragments that remain are able to contribute to improvements in mechanical properties via dityrosine formation.

SEM investigation of fibrin-based tissue revealed a dense matrix around the cell-deposited collagen fibrils (Figure 7 A and B). Coupled with fibrin/ogen immunostaining in Figure 5 and immunogold labeling shown in Figure 7 D and E, it is likely that the matrix around the collagen fibrils in this image contained residual fibrin fibrils, which serves to demonstrate the proximity of fibrils that could form dityrosine cross-links.

Suitable strength and stiffness are necessary attributes for acceptable engineered tissues but are of little value if they induce a strong inflammatory response upon implantation. This study examined subcutaneous implantation of cross-linked engineered tissue in a nude rat model to examine the effect of increased dityrosine on the innate immune response. Dityrosine presence in the body is common due to the action of activated phagocytes as a response to physiologic stressors, such as the presence of bacteria [31, 32], and it is almost exclusively excreted in urine when injected intravenously [31]. Results of this implant study revealed very low levels of inflammation for both cross-linked samples and controls, as shown in Figure 8.

This photo cross-linking method utilizes blue light ($\lambda$ = 458 nm), so that cytotoxic effects of UV exposure are avoided. Along with non-toxic levels of cross-linking chemistry, minimal cell death occurs after cross-linking [22, 24]. Though the viability was not quantified as a part of this study, Elvin et al. [22] and Syedain et al. [24] found minimal reduction in cell viability. Syedain et al. performed the cross-linking procedure on similarly prepared fibrin-based tissue constructs after either 1 day or 7 days of culture and then continued to culture the tissue for up to an additional 5 weeks. Comparing control to cross-linked tissue, similar cell densities were observed after 5 weeks of culture, and the cells were depositing collagen similarly on a per-cell basis [24].

Blue-light exposure also allows straightforward control of the degree of strength and stiffness achievable by modifying the exposure time. As shown in Figure 2 D and E, a maximum level in these mechanical properties was achieved after 10 seconds of exposure. Interestingly, these properties did not increase or plateau with longer exposure times. Rather, there was a clear decrease. However, this was not observed in control samples that were exposed to blue light for up to 60 seconds, rather the decrease only occurred in the presence of $[RuII(bpy_3)]^{2+}$ and SPS, implicating altered photochemistry at longer exposure times and not a detrimental effect of blue light on the ECM.

Though the experimentation here focused on vascular tissue engineering applications, there is potential for broader applications where greater strength and stiffness are required. Furthermore, this cross-linking method could be utilized to investigate materials other than fibrin/ogen-based tissue engineering, since tyrosine-rich molecules do not have to be present at the onset of tissue culture. Rather, cross-linking enhancements can be achieved at later culture times after ECM proteins have been deposited.

## Conclusions

A method of cross-linking completely biological, viable engineered tissue using a ruthenium-based chemistry and visible blue-light was presented. This method utilized tyrosine residues inherent to fibrin and cell-deposited proteins, yielding at least 3-fold mechanical strength increases and 10-fold stiffness increases after cross-linking, and these effects were able to be modified with culture duration prior to cross-linking or light exposure time. Both fibrin-based and collagen-based constructs demonstrated these effects. Cross-linked tissues were implanted subcutaneously and shown to have minimal inflammation after 30 days, similar to non-cross-linked controls. Overall, this cross-linking method is rapid, non-toxic, minimally inflammatory, and is capable of increasing stiffness and strength of engineered tissues to physiological levels.

## Supplementary Material

Refer to Web version on PubMed Central for supplementary material.

## Acknowledgments

The technical assistance of Naomi Ferguson, Ying Lung Lee and Lee Meier is gratefully acknowledged. Implantation procedures were conducted by Chad Burgess of University of Minnesota Experimental Surgical Services and histopathology was provided by Dr. George R. Ruth. This work was supported by the National Institutes of Health (NHLBI R01 HL083880 to RTT) and 3M Company (JWB). Parts of this work were carried out in the Characterization Facility, University of Minnesota, which receives partial support from NSF through the MRSEC program.

## References

1. Tsigkou O, Pomerantseva I, Spencer JA, Redondo PA, Hart AR, O'Doherty E, et al. Engineered vascularized bone grafts. Proc Natl Acad Sci U S A. 2010; 107(8):3311–6. [PubMed: 20133604]
2. Puppi D, Chiellini F, Piras AM, Chiellini E. Polymeric materials for bone and cartilage repair. Prog Polym Sci. 2010; 35(4):403–40.
3. Isenberg BC, Williams C, Tranquillo RT. Small-diameter artificial arteries engineered in vitro. Circ Res. 2006; 98(1):25–35. [PubMed: 16397155]
4. Syedain ZH, Weinberg JS, Tranquillo RT. Cyclic distension of fibrin-based tissue constructs: evidence of adaptation during growth of engineered connective tissue. Proc Natl Acad Sci U S A. 2008; 105(18):6537–42. [PubMed: 18436647]
5. Ahmed TAE, Dare EV, Hincke M. Fibrin: a versatile scaffold for tissue engineering applications. Tissue Eng Pt B-Rev. 2008; 14(2):199–215.
6. Grassl ED, Oegema TR, Tranquillo RT. Fibrin as an alternative biopolymer to type-I collagen for the fabrication of a media equivalent. J Biomed Mater Res. 2002; 60(4):607–12. [PubMed: 11948519]
7. Barocas VH, Tranquillo RT. An anisotropic biphasic theory of tissue-equivalent mechanics: the interplay among cell traction, fibrillar network deformation, fibril alignment, and cell contact guidance. J Biomech Eng. 1997; 119(2):137–45. [PubMed: 9168388]
8. L'Heureux N, Paquet S, Labbe R, Germain L, Auger FA. A completely biological tissue-engineered human blood vessel. FASEB J. 1998; 12(1):47–56. [PubMed: 9438410]
9. Charulatha V, Rajaram A. Influence of different crosslinking treatments on the physical properties of collagen membranes. Biomaterials. 2003; 24(5):759–67. [PubMed: 12485794]
10. Dong CM, Wu XY, Caves J, Rele SS, Thomas BS, Chaikof EL. Photomediated crosslinking of C6-cinnamate derivatized type I collagen. Biomaterials. 2005; 26(18):4041–9. [PubMed: 15626450]
11. Lew DH, Liu PHT, Orgill DP. Optimization of UV cross-linking density for durable and nontoxic collagen GAG dermal substitute. J Biomed Mater Res. 2007; 82B(1):51–6.
12. Cooper DR, Davidson RJ. The effect of ultraviolet irradiation on soluble collagen. Biochem J. 1965; 97(1):139–47. [PubMed: 16749094]

13. Girton TS, Oegema TR, Tranquillo RT. Exploiting glycation to stiffen and strengthen tissue equivalents for tissue engineering. J Biomed Mater Res. 1999; 46(1):87–92. [PubMed: 10357139]
14. Brinkman WT, Nagapudi K, Thomas BS, Chaikof EL. Photo-cross-linking of type I collagen gels in the presence of smooth muscle cells: mechanical properties, cell viability, and function. Biomacromolecules. 2003; 4(4):890–5. [PubMed: 12857069]
15. Sosnik A, Sefton MV. Semi-synthetic collagen/poloxamine matrices for tissue engineering. Biomaterials. 2005; 26(35):7425–35. [PubMed: 16023714]
16. Couet F, Rajan N, Mantovani D. Macromolecular biomaterials for scaffold-based vascular tissue engineering. Macromol Biosci. 2007; 7(5):701–18. [PubMed: 17477449]
17. Sell SA, Francis MP, Garg K, McClure MJ, Simpson DG, Bowlin GL. Cross-linking methods of electrospun fibrinogen scaffolds for tissue engineering applications. Biomed Mater. 2008; 3(4):1–11.
18. Dare EV, Griffith M, Poitras P, Kaupp JA, Waldman SD, Carlsson DJ, et al. Genipin cross-linked fibrin hydrogels for in vitro human articular cartilage tissue-engineered regeneration. Cells Tissues Organs. 2009; 190(6):313–25. [PubMed: 19287127]
19. Cornwell KG, Pins GD. Discrete crosslinked fibrin microthread scaffolds for tissue regeneration. J Biomed Mater Res. 2007; 82A(1):104–12.
20. Sosnik A, Leung B, McGuigan AP, Sefton MV. Collagen/poloxamine hydrogels: Cytocompatibility of embedded HepG2 cells and surface-attached endothelial cells. Tissue Eng. 2005; 11(11–12):1807–16. [PubMed: 16411826]
21. Fancy DA, Kodadek T. Chemistry for the analysis of protein-protein interactions: rapid and efficient cross-linking triggered by long wavelength light. Proc Natl Acad Sci U S A. 1999; 96(11):6020–4. [PubMed: 10339534]
22. Elvin CM, Brownlee AG, Huson MG, Tebb TA, Kim M, Lyons RE, et al. The development of photochemically crosslinked native fibrinogen as a rapidly formed and mechanically strong surgical tissue sealant. Biomaterials. 2009; 30(11):2059–65. [PubMed: 19147224]
23. Elvin CM, Danon SJ, Brownlee AG, White JF, Hickey M, Liyou NE, et al. Evaluation of photo-crosslinked fibrinogen as a rapid and strong tissue adhesive. J Biomed Mater Res. 2010; 93A(2): 687–95.
24. Syedain ZH, Bjork J, Sando L, Tranquillo RT. Controlled compaction with ruthenium-catalyzed photochemical cross-linking of fibrin-based engineered connective tissue. Biomaterials. 2009; 30(35):6695–701. [PubMed: 19782397]
25. Grassl ED, Oegema TR, Tranquillo RT. A fibrin-based arterial media equivalent. J Biomed Mater Res. 2003; 66A(3):550–61.
26. Ayad, S.; Boot-Handford, R.; Humphries, M.; Kadler, K.; Shuttleworth, A. The Extracellular Matrix Factsbook 2nd Ed. Academic Press; San Diego: 1998.
27. Isenberg BC, Tranquillo RT. Long-term cyclic distention enhances the mechanical properties of collagen-based media-equivalents. Ann Biomed Eng. 2003; 31(8):937–49. [PubMed: 12918909]
28. Starcher B. A ninhydrin-based assay to quantitate the total protein content of tissue samples. Anal Biochem. 2001; 292(1):125–9. [PubMed: 11319826]
29. Stegemann H, Stalder K. Determination of hydroxyproline. Clin Chim Acta. 1967; 18(2):267–73. [PubMed: 4864804]
30. Kim YJ, Sah RLY, Doong JYH, Grodzinsky AJ. Fluorometric assay of DNA in cartilage explants using Hoechst-33258. Anal Biochem. 1988; 174(1):168–76. [PubMed: 2464289]
31. Bhattacharjee S, Pennathur S, Byun J, Crowley J, Mueller D, Gischler J, et al. NADPH oxidase of neutrophils elevates o,o '-dityrosine cross-links in proteins and urine during inflammation. Arch Biochem Biophys. 2001; 395(1):69–77. [PubMed: 11673867]
32. Nowak P, Zbikowska HM, Ponczek M, Kolodziejczyk J, Wachowicz B. Different vulnerability of fibrinogen subunits to oxidative/nitrative modifications induced by peroxynitrite: functional consequences. Thromb Res. 2007; 121(2):163–74. [PubMed: 17467041]
33. Neidert MR, Lee ES, Oegema TR, Tranquillo RT. Enhanced fibrin remodeling in vitro with TGF-beta 1, insulin and plasmin for improved tissue-equivalents. Biomaterials. 2002; 23(17):3717–31. [PubMed: 12109697]

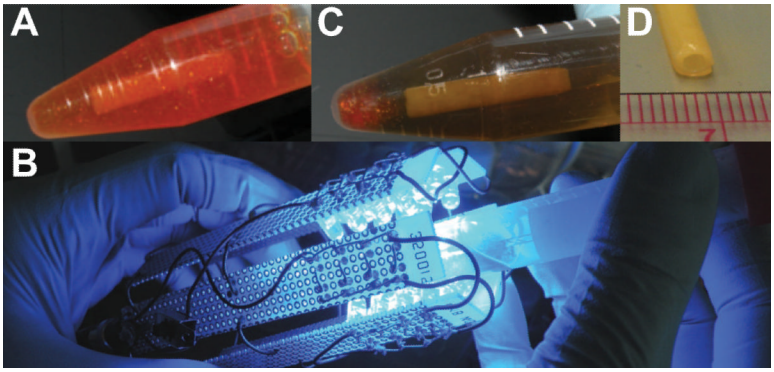


**Figure 1.**

Photo-cross-linking method. A: Tubular tissue construct maintained on a glass mandrel and incubated in the $[RuII(bpy)_3]^{2+}$ solution. B: The tissue is exposed to blue light in a custom blue-light LED mesh. After exposure, a clear change is apparent in the cross-linking solution (C) and the tissue opacity (D).

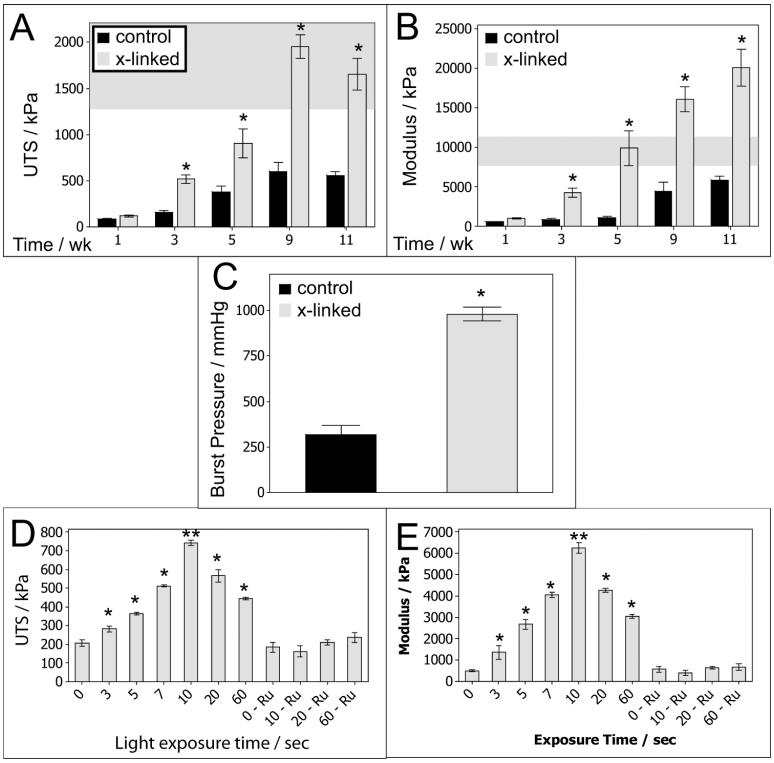


**Figure 2.**

Mechanical properties of cross-linked fibrin-based tissue. UTS (A) and young's modulus (B) for tissue harvested at varying weeks of culture ranging from 1 to 11 weeks. N = 7–9. (*) indicates $p < 0.05$ for a pair-wise comparison at that given time point in culture. The shaded region indicates native properties (mean ± σ) based on measurements of abdominal aorta [33]. C: Burst pressure for 9–11 week constructs. Mean burst pressures were 980 mmHg (cross-linked) vs. 318 mmHg (control). N = 6. UTS (D) and modulus (E) of 4-week tissue treated with varying blue-light exposure time. N = 8. Values for exposure times were higher than controls (zero light exposure controls and light exposure with no $[RuII(bpy_3)]^{2+}$ and SPS controls, $p < 0.05$ as indicated by *). The 10-second exposure time was significantly higher than all other points (as indicated by **)

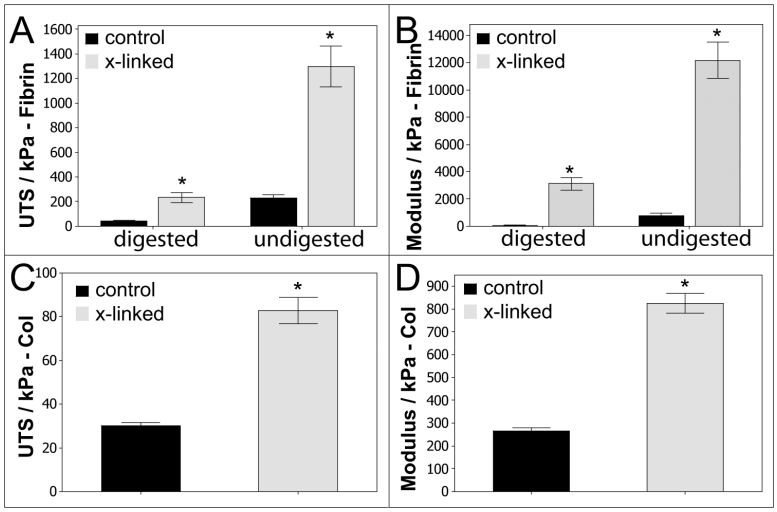


**Figure 3.**

Mechanical properties of trypsin-digested fibrin-based tissue and collagen-based tissue. UTS (A) and modulus (B) for trypsin-digested fibrin-based tissue. N = 3–4. UTS (C) and modulus (D) for collagen-based tissue. N = 8, $p < 0.05$ as indicated by *.

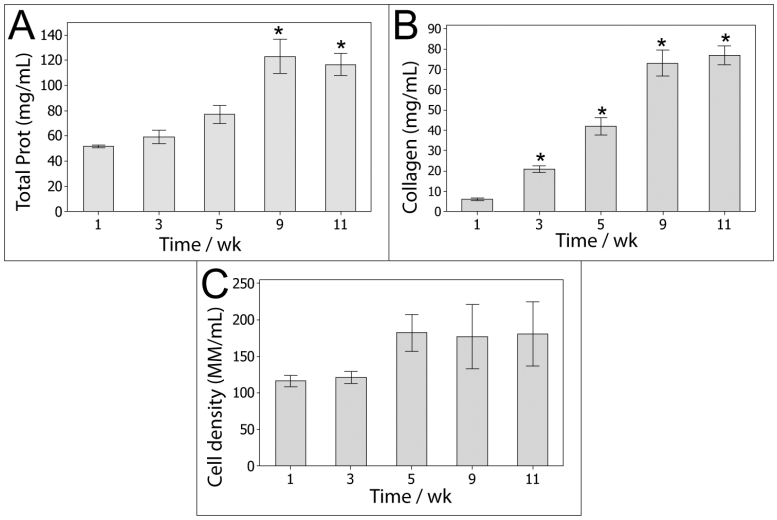


**Figure 4.**

Protein and cell density for fibrin-based tissue (initial gels consist of 3 mg/mL fibrin and contain no collagen). A: total protein concentration. B: collagen concentration. C: cell density. N = 4, * indicates $p < 0.05$ compared to 1-week levels.

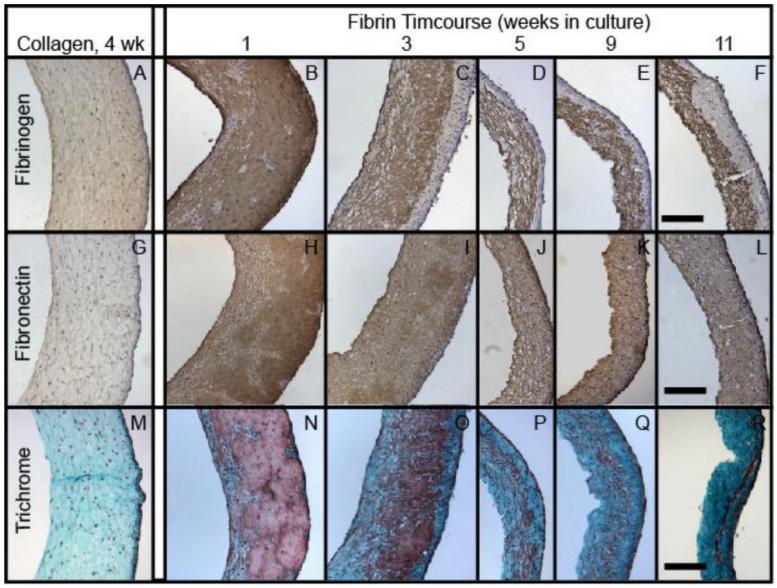


**Figure 5.**

Immunohistochemistry for fibrinogen (DAB, top row) and fibronectin (DAB, middle row), and Lillie's trichrome staining (bottom row). The left-most column consists of collagen-based engineered tissue harvested after 4 weeks. The remaining images are for fibrin-based tissue, showing (from left to right) samples harvested at 1, 3, 5, 9, and 11 weeks. All images have the lumenal edge facing the left pane and scale bar = 250 μm.

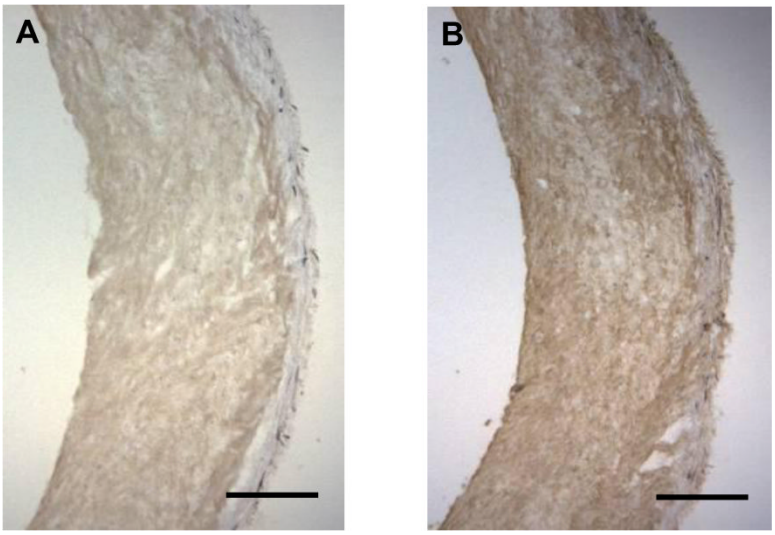


**Figure 6.**
DAB immunostaining of fibrin-based tissue samples after 4 weeks of culture and subsequently digested in trypsin overnight prior to cross-linking. A: Positive staining for fibrin/ogen. B: Positive staining for fibronectin. Scale bar = 250 μm.

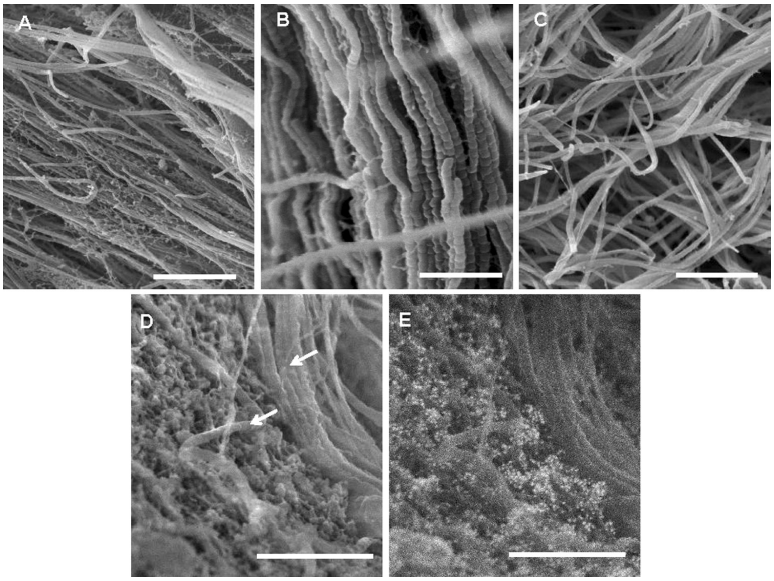


**Figure 7.**

SEM images of tissue constructs. A: Fibrin-based tissue after 5 weeks of culture with cell-deposited collagen fibers surrounded by residual fibrin and/or other deposited ECM in the sample fracture plane (scale bar = 850 nm), B: Higher magnification of fibrin-based construct showing cell-deposited, aligned collagen fibrils (scale bar = 370 nm), C: Collagen-based tissue after 4 weeks of culture. Interstitial matrix was sparse in collagen-based tissue compared to fibrin-derived tissue (scale bar = 850 nm). D: SEM image of a 4-week fibrin-based construct showing collagen fibers (arrows) surrounded by protein matrix. Scale bar = 430 nm. E: Backscatter electron image after labeling with anti-fibrinogen antibodies that were conjugated to 12 nm gold particles. Scale bar = 430 nm.

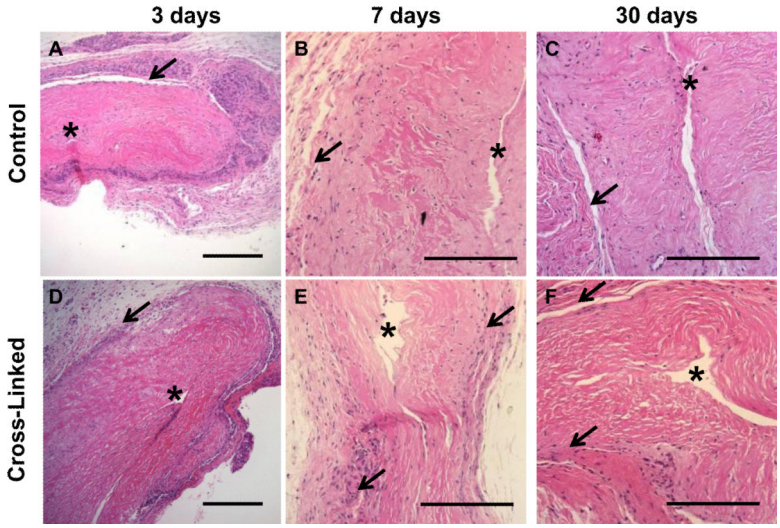


**Figure 8.**

H&E histopathology of subcutaneously implanted, 7-week fibrin-based tissue. A, D: At 3 days, there was a high density of inflammatory cells at the insertion site around the implanted tissue. Scale bar = 250 μm. B, E: By 7 days, the inflammation was significantly reduced. There was relatively little inflammation for both control and cross-linked tissues. Scale bar = 200 μm. C, F: By 30 days, inflammation was further reduced, with a thin layer of cells having fibroblast-like morphology surrounding the tissue constructs. Scale bar = 200 μm. For all images, the asterisk (*) denotes the lumen and arrows demarcate the interface of engineered tissue and host tissue.